Subinertial variability in the flow through the Strait of Gibraltar

J. García Lafuente,[1] E. Álvarez Fanjul,[2] J. M. Vargas,[1] and A. W. Ratsimandresey[2]

Received 16 August 2001; revised 20 February 2002; accepted 7 March 2002; published 24 October 2002.

[1] Current meter observations collected within Canary Azores Gibraltar Observations (CANIGO) project have been analyzed in order to study subinertial flows through the Strait of Gibraltar. Estimated net flow has been compared with hindcasts provided by Nivmar Prediction System-Hamburg Shelf Ocean Model (HAMSOM) circulation model forced by wind stress and atmospheric pressure applied to the North Atlantic Ocean and the Mediterranean Sea. The model was first run-forced by atmospheric pressure and then by atmospheric pressure and wind stress in order to assess the relative importance of each external agent on the subinertial flow. The main driving force is the atmospheric pressure over the Mediterranean Sea, although wind stress in the Atlantic side of the strait may contribute appreciably to subinertial net flow. Inflow variations account for 60% of the subinertial variability approximately. The interface depth correlates well with the net flow fluctuations, sinking or rising under positive (toward the Mediterranean) or negative fluctuations, respectively, with an average gain of around −60 m/Sv. These results have been interpreted in the scope of the hydraulic two-layer theory to conclude that the exchange is submaximal rather than maximal. Salinity on the interface increases (decreases) for positive (negative) net flow fluctuations. This is explained in terms of increased (decreased) recirculation of water from the passive Mediterranean layer driven by the velocity changes that atmospheric forcing induces in the active Atlantic layer. The contribution of the recirculated water to the fluctuations of the net flow is of secondary importance (around 5% on average), but the layer that recirculates may be thicker than 50 m, what could have important biological implications. *INDEX TERMS:* 4504 Oceanography: Physical: Air/sea interactions (0312); 4255 Oceanography: General: Numerical modeling; 4243 Oceanography: General: Marginal and semienclosed seas; 4235 Oceanography: General: Estuarine processes; *KEYWORDS:* Mediterranean Sea, Gibraltar Strait, hydraulic control, recirculation, atmospheric forcing

Citation: García Lafuente, J., E. Álvarez Fanjul, J. M. Vargas, and A. W. Ratsimandresy, Subinertial variability in the flow through the Strait of Gibraltar, *J. Geophys. Res.*, *107*(C10), 3168, doi:10.1029/2001JC001104, 2002.

1. Introduction

[2] The Strait of Gibraltar, connecting the Atlantic Ocean with the Mediterranean Sea through a rather complicated system of sills and narrows, is the scenario of a well-studied baroclinic exchange driven by the net evaporative losses within the Mediterranean Sea. A long term averaged net (also known as barotropic) flow of the order of $\overline{Q_0} = 0.05$ Sv (Sverdrup, 1 Sv = 10^6 m^3s^{-1}) is necessary to compensate for the evaporation in the Mediterranean. This net flow $\overline{Q_0}$ is the difference of two quantities $\overline{Q_1}$ and $\overline{Q_2}$, the inflow and outflow, respectively, which are one order of magnitude greater.

[3] The exchange is not steady but highly variable. According to the timescale of the process under study this variability has been traditionally classified into tidal, subinertial, which is driven mainly by meteorological forcing, and long term (seasonal and interannual). There are interactions between these scales. For instance, positive correlation between tidal currents and interface oscillations in the main sill of Camarinal (Figure 1) contributes by more than one half to the mean exchange $\overline{Q_1}$ and $\overline{Q_2}$ [*Bryden et al.*, 1994].

[4] It has been recognized from long ago that atmospheric pressure over a semienclosed basin forces a net flow through the connecting strait with the open ocean in order to adjust the basin to the new external forcing. *Crepon* [1965] observed a correlation between the flow through the Strait of Gibraltar and the atmospheric pressure over the Mediterranean Sea, rather than between the flow and the time derivative of the atmospheric pressure as conservation of volume would suggest. *Garrett* [1983] suggested that flows through the Strait of Sicily and differing sea levels in the eastern and western Mediterranean basins should be included in the analysis of the response. *Garrett and Majaess* [1984] applied these ideas to explain the nonisostatic response of the Eastern Mediterranean sea level to atmospheric pressure but they did not focus on the response of the

[1]Departamento de Física Aplicada II, University of Málaga, Málaga, Spain.
[2]Area del Medio Físico, Puertos del Estado, Madrid, Spain.

0148-0227/02/2001JC001104$09.00

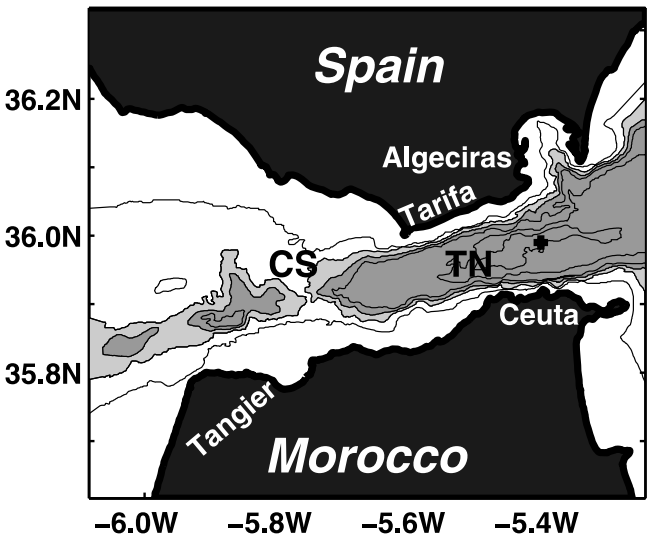

Figure 1. Map of the Strait of Gibraltar showing some topographic features. Isobaths have not been labeled for clarity. "CS" is Camarinal Sill, and "TN" is Tarifa Narrows. Isobath depths are 100, 200, 290 (to illustrate the depth of the sill), 400, 700, and 900 m. Depths greater than 290 m are in light grey shadow, and those greater than 400 m are in deep grey shadow. The cross indicates the position of the mooring line.

net flow through the straits to this forcing. *Candela et al.* [1989], presented a model that addressed explicitly this response. The predictions of this model improved considering the first empirical mode of the atmospheric pressure over the Mediterranean as the external forcing rather than the spatially averaged pressure. On the other hand, the model of *Candela et al.* [1989] did not take into account the wind field, nor the fluctuating atmospheric pressure over the Atlantic Ocean, this last assumption being justified in terms of the isostatic response of the Atlantic Ocean to travelling atmospheric systems. *Le Traon and Gauzelin* [1997] used the model of *Candela et al.* [1989] to explain the mean sea level variability of 3 years of TOPEX/Poseidon data of the Mediterranean Sea and found reasonable agreement between observed and predicted sea levels at subinertial frequencies. Also, they put forward a simple model to analyze the influence that variable atmospheric pressure in the Atlantic Ocean could have on the subinertial fluctuations of sea level in the Mediterranean Sea. The new explained variance was close to, but less than, that explained without taking the atmospheric pressure over the Atlantic Ocean into account and they concluded that this pressure should play a minor role in the subinertial variability of the net flow.

[5] The aforementioned works deal with the net flow fluctuation but did not address the important question of the response of the baroclinic exchange to the externally forced barotropic fluctuation. This problem was first analyzed by *Farmer and Armi* [1986] within the scope of the two-layer hydraulic control theory. This theory predicts maximal exchange if the two-layered flow is controlled at two sections connected by a subcritical region. The candidate locations for control are the narrowest section off Tarifa (see Figure 1) and the section of minimum cross area of Camarinal Sill. *Farmer and Armi* [1986] incorporated the fluctuating barotropic signals into the model using a quasi-steady approximation in which the steady solution is verified at each point of the cycle. Figure 16 of *Farmer and Armi*'s [1986] paper show that for moderate net flows and maximal exchange, inflow and outflow fluctuations contribute half and half to the net flow fluctuation very approximately. The same result was obtained by *Delgado et al.* [2001].

[6] While the actual exchange is a two way exchange, it is not a two-layer exchange in the sense of two layers of homogeneous properties. Mixing and water entrainment originate a transitional layer in which properties of the flow like density or water speed changes gradually. Despite of this fact, there is still a tendency to interpret the observations in a two-layered model, the properties of either layer being defined as depth averaged properties. A reason for this would be the success that the two-layer hydraulic theory has had in predicting some of the most outstanding internal features of the strait [*Armi and Farmer*, 1988]. There is also literature of three-layer exchange that includes that transitional layer of changing properties [*Bray et al.*, 1995; *Winters and Seim*, 2000].

[7] An interface definition is necessary to carry out a two-layer decomposition. The easier and more obvious definition is the surface of zero along strait velocity that separates water flowing into the Mediterranean and water flowing out. However, tidal currents are strong enough to reverse subtidal currents, making the flow unidirectional in many places of the strait during part of the tidal cycle [*Candela et al.*, 1990; *García Lafuente et al.*, 2000]. Other definitions would be necessary for analyzing the exchange at tidal frequencies. The usual choice is a surface of a certain salinity. *Bryden et al.* [1994] used $S = 37.0$ in Camarinal Sill, while *Candela et al.* [1990], considered $S = 37.2$ in the eastern section. *García Lafuente et al.* [2000] concluded that $S = 37.8$ was more adequate in this section after observing that this salinity surface maximized the mean exchanged flows. *Baschek et al.* [2001], following a similar approach, obtained $S = 38.1$ at this same section. If salinity observations are not available, then the surface of maximum vertical shear of horizontal velocity may be used to define the interface when flows reverse. This definition is particularly useful for analyzing data of acoustic Doppler current meter profilers [*Tsimplis and Bryden*, 2000]. Subinertial velocities only reverse in very exceptional situations of extreme meteorological forcing which may last 3 or 4 days at most. In these rare cases we would face again the problem of the interface definition, though these unusual events could be considered as brief events of arrested inflow or outflow. Seasonal and interannual fluctuations are always too weak to reverse flows and the surface of null velocity is a well-defined interface [*García Lafuente et al.*, 2002]. Thus, the surface of null along-strait velocity is appropriate to carry out an analysis of the two-way exchange at subinertial frequencies.

[8] This paper addresses the topics discussed above, namely the net flow response to external atmospheric forcing, including wind stress, and the response of baroclinic exchange to the net flow fluctuations. The first question is analyzed using the numerical barotropic model

described in Section 3 whose domain extends over most of the Mediterranean Sea and a large portion of the North Atlantic Ocean. The model includes wind forcing and variable atmospheric pressure over the Atlantic Ocean and represents a step forward in modeling the subinertial flow through the Strait of Gibraltar. The predictions (hindcasts, actually) of the model are compared in Section 4 with the net flow estimated from observations collected within CANIGO project, which have been previously presented in Section 2. Section 5 investigates the baroclinic response of the exchange to atmospheric forcing and discusses the results within the scope of the two-layer hydraulic theory. Regarding the study of fluxes of other biogeochemical properties, the use of a material interface like a salinity interface along with the interface of null velocity provides a tool to investigate water recirculation. This concept is bound to the fact that the vertical structure of the flow is not two-layered and that the net barotropic fluctuations mismatches these two interfaces in the sense that the salinity in the surface of null velocity changes following the fluctuations of the net flow [*García Lafuente et al.*, 2000]. This issue is also addressed in Section 5. Section 6 summarizes the results of our analysis and presents the conclusions.

2. Data and Methods

[9] From October 1995 to May 1998 a mooring array of recording current meters was deployed in the eastern part of the Strait of Gibraltar within CANIGO project to help resolve the different timescales of the exchange. A complete description of this data set is given by *García Lafuente et al.* [2002]. In the present study only the period from October 26, 1997, to March 30, 1998, has been considered. It contains the most complete current meter observations in the central mooring (see Figure 1), which is the key place to estimate the exchange at the eastern section. Nominal depths of the five instruments that worked properly were −40, −70, −140, −200, and −550 m (two other instruments situated at −360 and −800 m depth did not work). Instruments had conductivity cells to evaluate salinity. Corrections necessary to compensate for the biological contamination of conductivity cells were made in the manner explained by *García Lafuente et al.* [2000].

[10] Relatively strong lower layer tidal currents acting upon the line wire pushed instruments down, so they sometimes registered at depths different from the nominal one. Every observation of velocity and salinity is accompanied by the depth at which the instrument was (as measured by the pressure sensor mounted on the instrument). This depth has been used to interpolate salinity and velocity along the z axis.

[11] Subinertial series were obtained after removing the tidal contribution of species 1 and 2 according to the procedure explained by *García Lafuente et al.* [2000]. Finally, all series were filtered with a Gaussian-like filter of 1 cpd cutoff frequency and subsampled to two values per day.

[12] Time dependent subinertial water transports $Q_1(t)$ and $Q_2(t)$ were computed according to

$$Q_1(t) = \int_y \int_{h_2(y,t)}^{0} u(y,z,t)\,dz\,dy \qquad (1)$$

$$Q_2(t) = \int_y \int_{bottom(y)}^{h_2(y,t)} u(y,z,t)\,dz\,dy \qquad (2)$$

where $h_2(y, t)$ is the depth of the interface at instant t and $u(y, z, t)$ is the along-strait velocity. The Cartesian reference system has been rotated +17° in order to have the x axis oriented along strait. The y axis points to the north shore and the z axis is positive upwards with origin at the sea surface.

[13] In practice, equations (1) and (2) must be computed numerically from observations taken with a single mooring that do not resolve the cross-strait structure of the flow nor its vertical structure satisfactorily. Thus, there are some questions facing the computation. First, there is the lack of observations in the 40 or 50 upper meters of the water column. This shallow layer has been historically missed by field experiments for technical and operational reasons, making the long-term inflow to be poorly determined from direct observations [*Bryden et al.*, 1994; *García Lafuente et al.*, 2000; *Baschek et al.*, 2001]. To partially resolve this question, velocities above the depth of the upper instrument have been linearly extrapolated. The filter rule of $u = 2$ ms^{-1} at $z = -5$ m has been used whenever the extrapolated velocity at this depth exceeded 2 ms^{-1} in order to avoid unrealistic high values. The rule was applied after checking that 2 ms^{-1} was an actual upper limit of the whole CANIGO observations in the eastern section. This extrapolation that is almost certainly the main source of error in the estimate of $Q_1(t)$ is further addressed in the next paragraph. An interpolated/extrapolated velocity every 10 m from the bottom to the surface was obtained to compute equations (1) and (2).

[14] Second, we have to assume that horizontal velocities at the sampling depths in the center of the strait are representative for the whole section at these depths. The spatial structure of the mean flow shown by *Send et al.* [1999] and analyzed in detail by *Baschek et al.* [2001] indicates that this is not the case. Absolute velocities in the eastern section are systematically greater in the central part of the strait, diminishing shorewards. Considering the velocity in the center for the whole section leads to flow overestimates that have been compensated by shrinking the actual cross-strait area of the 10 m thick bins associated with every interpolated value of the velocity. The reduction was proportional to the distance of the bin to the seafloor according to the law $(1 - (700 + z)/A)^n$, for -700 m $< z < 0$ m. Cross-areas were not reduced below -700 m. Parameter A was set to 10^4 m arbitrarily and the power of the weighting function was adjusted by imposing the new constraint that the time-averaged net flow was null. Actually, $\overline{Q_0} \sim 0.05$ Sv but tidal and subinertial fluctuations may be orders of magnitude greater [*Candela et al.*, 1989; *Bryden et al.*, 1994; *García Lafuente et al.*, 2000]. This is why it is not unusual to ignore $\overline{Q_0}$ when studying higher frequency processes. Moreover, the net flow has a seasonal signal of around 0.1 Sv of amplitude with minimum in March [*García Lafuente et al.*, 2002]. Since the time series spans over winter, $\overline{Q_0} = 0$ becomes a realistic assumption. More importantly, this constraint put limits to the uncertainties in the estimates of $Q_1(t)$, linking its mean value to the mean value of $Q_2(t)$, which is usually more accurately determined. The overall area was reduced by 80% approx-

imately, though the reduction reached 65% at the depth of the shallowest instrument. The correction that this reduction causes in the central-mooring-line-based computed flows is compatible with the cross-strait velocity structure presented by *Baschek et al.* [2001].

[15] Finally, two type of interfaces have been worked to compute equations (1) and (2): the surface of null along-strait velocity, well defined throughout the period except for 3 to 4 days in February 1998, and surfaces of a prescribed salinity. Their depths have been computed by linear interpolation of velocity or salinity observations. Transports computed according to the first criterion are named $Q_{1U}(t)$ and $Q_{2U}(t)$) and referred as to inflow and outflow, respectively. They include all water flowing in (out) the Mediterranean regardless its T-S characteristics. Transports computed according to the second definition are related to the advection of salt associated with water masses but they might also be related to other solved and suspended substances. They depend on the value of salinity S_i used to compute equations (1) and (2). In order to find the best salinity interface, time-averaged transports from $S_i = 36.8$ to $S_i = 38.1$ at steps $\Delta S = 0.1$ have been calculated. They fit a fourth degree polynomial of S almost perfectly ($r^2 = 0.99$), from which the S coordinate that maximizes $\overline{Q_{1S_i}}$ and $|\overline{Q_{2S_i}}|$ has been obtained. The surface $S = 37.77$ verified this condition and is the best material interface during the period of observations. Names $Q_{1S}(t)$ and $Q_{2S}(t)$ have been reserved for this particular interface and they are called upper and lower layer transports hereinafter. While $Q_{1U}(t)$ is always positive (or $Q_{2U}(t)$ always negative), $Q_{1S}(t)$ or $Q_{2S}(t)$ can change sign if the layer reverses. Note also that the net flow is independent of the choice of the interface ($Q_0(t) = Q_{1U}(t) + Q_{2U}(t) = Q_{1S_i}(t) + Q_{2S_i}(t)$).

[16] The time-averaged inflow (outflow) obtained after applying the above described method is 0.75 Sv, whereas the time averaged upper and lower layer transport is 0.73 Sv, very close indeed. The method did not aimed at doing accurate estimates of the mean exchanged flows but at estimating subinertial fluctuations. It is encouraging, however, to see that the mean value is within the error interval of recent estimates made during CANIGO, such as those given by *Baschek et al.* [2001] (-0.76 ± 0.07 Sv and 0.81 ± 0.07 Sv for outflow and inflow, respectively) or by *Tsimplis and Bryden* [2000] (-0.67 ± 0.26 Sv and 0.78 ± 0.47 Sv). This good agreement (within ±10%) is important since similar statistical confidence can be assumed for the computed subinertial fluctuations $Q_0(t)$, which are shown in Figure 2.

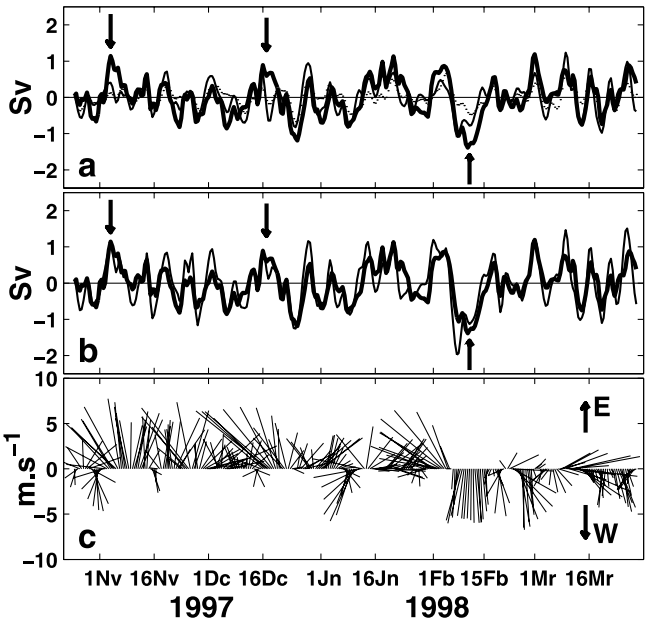

Figure 2. (a) Computed net flow (thickest line), hindcast net flow when NPS model is uniquely forced by atmospheric pressure (thick line), and net flow predicted by the model of *Candela et al.* [1989] (thin line). (b) Computed net flow (thick line) and NPS net flow hindcast by the model forced with atmospheric pressure and wind stress (thin line). (c) Stick diagram of spatially averaged wind velocity over the Gulf of Cadiz, west of the Strait of Gibraltar. East and west directions have been marked. Arrows in Figures 2a and 2b indicate events of net flow fluctuations that are not adequately hindcast if wind stress is not included in the forcing terms, but that are if it is included.

3. Numerical Model

[17] The numerical model used by Nivmar Prediction System (NPS) [*Álvarez Fanjul et al.*, 2001] has been applied to hindcast the meteorologically forced flow through the Strait of Gibraltar during the period of observations. The NPS uses the Hamburg Shelf Circulation Model (HAMSOM) circulation model [*Backhaus*, 1983; *Backhaus and Hainbucher*, 1987; *Álvarez Fanjul et al.*, 1997] forced by atmospheric pressure and wind fields. NPS has been designed for sea level (tide and storm surge) forecasts. However, since the domain of integration includes the Mediterranean Sea and the North Atlantic Ocean (see Figure 3), the model computes the barotropic (net) flow through the Strait of Gibraltar as an added value output.

[18] The HAMSOM model is a three dimensional multilevel (z coordinate) finite difference model (Arakawa C grid) based on the barotropic set of Reynolds equations. NPS uses the vertically integrated HAMSOM model that solves the equations:

$$u_t + uu_x + vu_y - fv + g\eta_x = \frac{\tau_w^{(x)}}{\rho H} - \frac{\tau_b^{(x)}}{\rho H} - \frac{P_{Ax}}{\rho} + \mu\nabla^2 u \qquad (3)$$

$$v_t + uv_x + vv_y + fu + g\eta_y = \frac{\tau_w^{(y)}}{\rho H} - \frac{\tau_b^{(y)}}{\rho H} - \frac{P_{Ay}}{\rho} + \mu\nabla^2 v \qquad (4)$$

$$\eta_t + (Hu)_x + (Hv)_y = 0 \qquad (5)$$

where (u, v) are the components of depth-integrated mean velocity, $H = h + \eta$ is the total water depth, η is the surface elevation relative to the undisturbed water depth h, f is the Coriolis parameter, g is the gravitational acceleration, ρ is the water density, $\tau_w^{(x,y)}$ and $\tau_b^{(x,y)}$ are wind stress and bottom stress, respectively, μ is the horizontal eddy viscosity and P_A is the atmospheric pressure. Bottom stress is parameterized by the quadratic law:

$$\vec{\tau_b} = C_b \rho |\vec{u}| \vec{u} \qquad (6)$$

where C_b is the dimensionless drag coefficient.

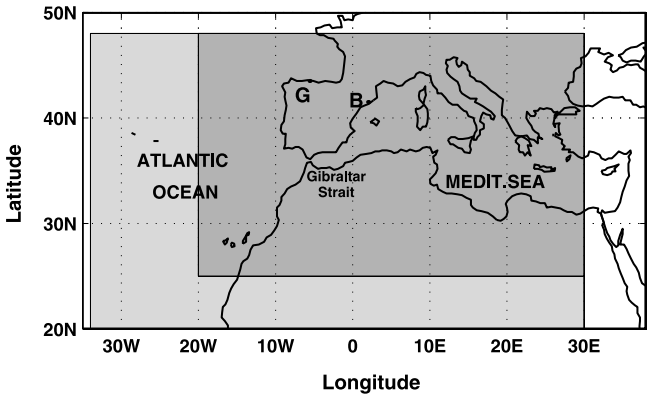

Figure 3. Domain of the numerical model (shaded rectangles). The smaller darker grey rectangle is the region of constant grid size. Barcelona (B) and Gijon (G), which are two of the locations used to tune the model coefficients, have been marked in the map.

[19] The model domain (Figure 3) is 20°N to 48°N and 34°W to 30°E. It uses a variable grid size scheme based on a zooming technique in order to reduce the computation time. The region from 25°N to 48°N and from 20°W to 30°E has a constant resolution of $15' \times 10'$ (*longitude* × *latitude*). The grid size in the rest of the domain increases progressively toward the boundaries by a factor of roughly 1.1 with respect to its inner neighbor. At the model resolution the strait is represented by a single grid point, which provides a quite realistic width of $10'$ or 18.5 km. The bottom depth in this point was set to 160 m so that the model cross-strait area equals the actual cross area of Camarinal Sill, the bottleneck of the Strait of Gibraltar.

[20] The atmospheric external forcing consisted of wind and sea level atmospheric pressure with spatial-temporal resolution of $30' \times 30'$ and 6 hours generated by the Spanish Meteorological Office through the operational application HIRLAM. Forcing fields were interpolated linearly in time and bilinearly in space. Wind stress was computed from wind fields using the Charnock parameterization [*Charnock*, 1955] with $\alpha = 0.032$, this value being selected after some tuning [*Álvarez Fanjul et al.*, 1998].

[21] Nonslip boundary conditions were imposed in the solid walls of the domain. Sea level in the Atlantic open boundaries was corrected for atmospheric pressure according to the inverse barometer effect. In the Mediterranean Sea, the atmospheric model only reaches 30°E, leaving a small portion of the Eastern Mediterranean outside the domain. Thus, the NPS model should handle another open boundary. It is because the inverse barometer correction is not satisfactory within the Mediterranean Sea [*Garrett and Majaess*, 1984; *Le Traon and Gauzelin*, 1997] that a fictitious solid wall was placed at 30°E. The omission of part of the Levantine Basin could have some effects on the hindcast barotropic fluctuations through the strait. There are reasons, however, to think that the influence is not important. While general circulation 3-D models of the Mediterranean cannot ignore this Basin, one of the most important areas (if not the most) for the deep convection that drives the thermohaline circulation of this Sea, a barotropic 2-D model driven by mechanical forces is not much sensitive to this climatic forcing. The effect of the omission of part of the Levantine Basin in NPS would be simply proportional to the 10% of the surface of the Mediterranean that it represents, at most. Moreover, it is the furthest basin from the Strait of Gibraltar and whatever its influence might be it almost certainly has damped out well before reaching the surroundings of the strait. Again, this will not be true for general 3-D circulation models taking into account the expected relationship between the outflow through the Strait of Gibraltar and the deep water formation processes.

[22] Modelled flows depend on the horizontal friction and bottom drag coefficients. Horizontal eddy viscosity coefficient, μ, has been chosen proportional to the grid size, following the ideas behind *Schwiderski*'s [1980] formulation. Bottom drag coefficient was set to $C_b = 0.0025$, a rather typical value, and $\mu = 200\ m^2 s^{-1}$ in the region where the grid size was constant (see Figure 3). These values were selected during the tuning process of the model in order to match the sea surface elevation at several tide gauge locations around Spain. It is important to remark that the main objective of the tuning process (also of the NPS) was to reproduce correctly the sea levels around the Spanish coasts, including obviously the area of the Strait of Gibraltar, but not to optimize the correlation with $Q_0(t)$ computed from the observations.Correlation between predicted and observed sea levels in the Spanish ports of Barcelona and Gijon (Mediterranean and Atlantic coasts, respectively, see Figure 3) was higher than 0.85. Accordingly, baroclinic contribution to sea level, which is not included in the NPS barotropic model, is of minor importance, as expected. On the other hand, this high correlation suggests that the net flow computed by the model should be quite realistic in spite of the low spatial model resolution at the strait.

[23] Another point worthy to be commented is the numerical value of μ. During the model tuning, hindcast sea levels showed to be not much sensitive to μ (in terms of correlation and RMSE) unless unrealistic high values were used. The question arises as whether $200\ m^2 s^{-1}$ is unrealistically high or not. The nonslip condition imposed in the solid boundary implies that the largest value of $\mu\nabla^2 u$ will be achieved in the point representing the strait, where the term would be $8\mu D^{-2}u$, D being the strait width in the model. Actually the viscous term in this particular point is equivalent to a linearized lateral friction of the form λu, widely used in simple exchange models [*Garrett*, 1983; *Candela et al.*, 1989], with $\lambda = 8\mu D^{-2} = 4.6 \times 10^{-6}\ s^{-1}$, a quite reasonable value. Time series produced by the model have been filtered with a filter of the same cutoff frequency as the filter used in the data processing and decimated to the same sampling interval of 0.5 days.

4. Net Flow Fluctuations

4.1. Fortnightly Cycle

[24] The main contributor to the variance of the net flow time series of Figure 2 is the atmospheric forcing because high frequency tidal variability has been filtered out previously to the computation of $Q_0(t)$ and seasonal and interannual variability cannot introduce much variance in a 6 months long time series. The possibility exists, however, that low frequency tidal constituents, particularly M_{sf},

account for some variance. Since this fortnightly signal is astronomic rather than meteorological, its presence in $Q_0(t)$ may obscure the atmospheric forcing.

[25] To address this question, a fortnightly sinusoidal signal was generated and least squares fitted to $Q_0(t)$. The amplitude provided by the fitting was 0.18 ± 0.08 Sv and the phase (referred to full moon) was $140 \pm 22°$, maximum net flow (toward the Mediterranean Sea) occurring around 1 day before neap tides. However, the correlation coefficient is so small ($r^2 = 0.10$) that $Q_0(t)$ was assumed to remain unaffected by the fortnightly tide. Consequently, it has not been corrected for this signal. Our finding conflicts with the results that *Tsimplis and Bryden* [2000] obtained from ADCP data collected in Camarinal Sill. They found an intense fortnightly cycle in the inflow, a noticeably smaller signal in the outflow and, therefore, a very clear signal in the net flow, peaking around 1 day after neap tides. No explanation are put forward for this discrepancy, though it must be noted that both data sets do not span the same period.

4.2. Model Hindcasts

[26] In a first run, wind stress was not included in the forcing terms of NPS model in order to evaluate the effect of the atmospheric pressure alone. The run output can be compared with the prediction of the much simpler analytical model of *Candela et al.* [1989]. Both predictions are shown in Figure 2a. The correlation coefficient between $Q_0(t)$ estimated from the data and the prediction of Candela's model is $r = 0.66$. Candela (personal communication) found very similar correlation using longer time series of $Q_0(t)$ computed in Camarinal Sill, suggesting that Figure 2a is representative of the performance of this model. The correlation coefficient between $Q_0(t)$ and the hindcasts of NPS model hardly exceeds that figure ($r = 0.70$) in spite of the higher complexity of the latter. The correlation between both models, $r = 0.77$, is not so high as might be expected considering that they are forced by the same and unique external agent.

[27] The correlation coefficient between modelled and observed time series raises up to $r = 0.80$ when wind stress is included in the forcing terms of NPS model (Figure 2b). The comparison of Figures 2a and 2b suggests that the main effect of wind stress is to amplify the response of the flow induced by atmospheric pressure and therefore both hindcasts are well correlated ($r = 0.89$). However, there are also remarkable differences between the two predictions during specific periods, the wind stress improving the prediction (see arrows in Figures 2a and 2b). Figure 2c shows that the spatially averaged wind over the Gulf of Cadiz and Alboran Sea on the dates marked with arrows was favorable for establishing the appropriate sea level set up and, hence, the additional along-strait pressure gradient necessary to bring the estimated and modelled net flows closer to each other. Direct wind dragging might have contributed to improve the agreement too. Probably both mechanisms have been acting simultaneously.

[28] The aforementioned discussion indicates that local wind stress can be important in determining the net flow during some particular events. To test whether this correlation stands in general, the difference between the output of the model run forced by atmospheric pressure and wind stress and the run forced by atmospheric pressure alone was computed. Reasonably, this difference is a measurement of wind stress contribution to the net flow. The correlation coefficient between this contribution and the component of wind stress along the main principal axis of the spatially averaged wind stress in the Gulf of Cadiz is $r = 0.60$. The correlation drops below $r = 0.40$ if wind stress in the Alboran Sea is included in the average and it drops even more if only wind stress over the Alboran basin is taken into account. It is wind forcing over the Atlantic side of the strait rather than over the side of the semienclosed Mediterranean Sea that appears to influence the net flow fluctuations in the strait, the wind setup of sea level being the likely mechanism as mentioned earlier.

5. Baroclinic Response

[29] The second topic analyzed in this paper is the baroclinic response of the exchanged flow to meteorologically induced barotropic fluctuations. The NPS model is only marginally useful in this analysis because of its barotropic nature.

5.1. Inflow and Outflow Contribution to the Net Transport

[30] Time series of inflow ($Q_{1U}(t)$) and outflow ($Q_{2U}(t)$) are shown in Figure 4a. Mean and fluctuating parts have been separated out according to $Q(t) = \overline{Q} + q(t)$. The constraint of zero time-averaged net flow $\left(\overline{Q_0} = 0\right)$ implies that $Q_0(t) = q_{1U}(t) + q_{2U}(t)$. These fluctuating parts, which are the inflow and outflow response to the externally imposed barotropic fluctuation, have a marked tendency to oscillate in phase and in phase with $Q_0(t)$ too (Figure 4b), $q_{1U}(t)$ oscillating with higher amplitude on average than $q_{2U}(t)$. The enhanced response of $q_{1U}(t)$ could be related to wind dragging on the upper layer. The relatively good correlation ($r = 0.59$) between $q_{1U} - q_{2U}$ and the zonal wind stress would support this hypothesis. Barotropic fluctuations force interface oscillations as well. Figure 5 shows how the position of the interface of null along-strait velocity follows quite well the observed barotropic fluctuations. Figure 6 is the scatterplot of the interface depth against Q_0. The slope of -60 ± 2m/*Sv* of the fitted line ($r = -0.85$, $P < 0.0001$) could be interpreted as a subinertially averaged gain function.

[31] It is interesting to compare these results with the predictions of the two-layer hydraulic control theory. It was already mentioned in the Introduction that, under maximal exchange, this theory predicts almost equal contributions of inflow and outflow ($q_{1U}(t) \sim q_{2U}(t)$) to moderate barotropic fluctuations $Q_0(t)$ [*Farmer and Armi*, 1986; *Delgado et al.*, 2001]. In this case, the variance of either $q_{1U}(t)$ or $q_{2U}(t)$ should be one fourth of the variance of $Q_0(t)$. Figure 4b suggests that this is not the case: the variance of $q_{1U}(t)$ is 65% higher than predicted and the covariance of $q_{1U}(t)$ and $q_{2U}(t)$ drops more than 40% below its predicted value. Inflow variability is enhanced with regard to outflow variability and contributes by 59% to net flow variability. On the other hand, *Delgado et al.* [2001], following a model proposed by *Bormans and Garrett* [1989] and using a realistic topography of the strait, computed the response of the interface to imposed barotropic fluctuations. In the eastern section where the observations were made, the dependence was almost lineal for a wide range of values of Q_0. In

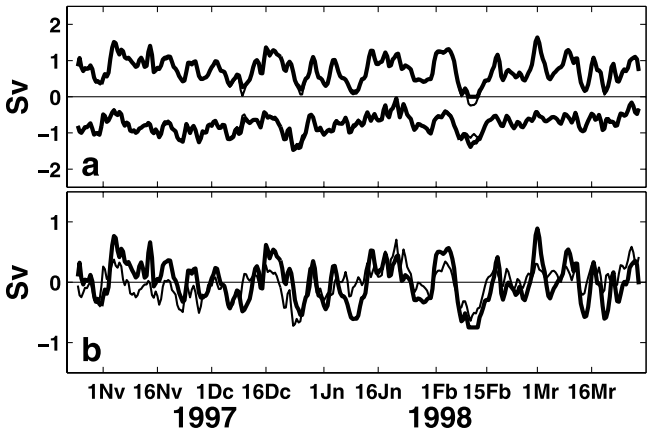

Figure 4. (a) Time series of inflow $Q_{1U}(t)$ and outflow $Q_{2U}(t)$ (thick lines) and upper $Q_{1S}(t)$ and lower $Q_{2S}(t)$ layer transports (thin lines) in a two-layer decomposition. (b) Time series of the fluctuating parts of inflow $q_{1U}(t)$ (thick line) and of outflow $q_{2U}(t)$ (thin line).

case of maximal exchange, the slope was −9 m/Sv, which is far from the value deduced from Figure 6.

[32] Submaximal exchange that happens when one (or both) control section does not exist, adds complexity to the analysis. The fact that Mediterranean water falls down to a depth of around 1000 m in the Atlantic Ocean [*Baringer and Price*, 1997], well below the sill depth of 290 m, suggests that Camarinal Sill is a permanent control section [*Garrett*, 1996]. It is the control section off Tarifa that would not exist in case of submaximal exchange. A new condition, like the depth of the interface in a point of the strait, must be prescribed to fully solve the problem [*Delgado et al.*, 2001]. Two results of interest concerning the discussion above are that inflow and outflow may fluctuate independently of each other and that the oscillations of the interface are enhanced with regard to the maximal exchange [*Delgado et al.*, 2001]. Specifically, for marginally submaximal exchange, a situation that corresponds to the transition from maximal to submaximal, the interface response is −31 m/Sv. Strictly submaximal exchange may modify this figure to the side of the observed value. Also, the fact that $q_1(t)$ and $q_2(t)$ do not have the same variance agrees with submaximal better than with maximal exchange.

5.2. Recirculated Water

[33] Figure 4a shows in thin line the time series of the upper and lower layer transports $Q_{1S}(t)$ and $Q_{2S}(t)$. They do not much differ from $Q_{1U}(t)$ and $Q_{2U}(t)$ but they are not the same. The most extreme difference happened in February 1998, when the inflow stopped during some days whereas the upper layer transport reversed during the same period. The substantially different description of the event is not contradictory but a consequence of the definition of flows and layer transports. Q_{1U} cannot be negative while Q_{1S} can be.

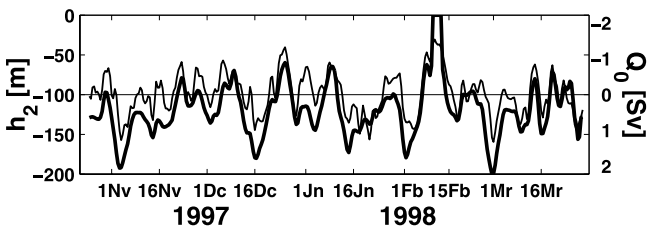

Figure 5. Time series of the depth of the interface (thick line, left scale) and of barotropic transport (thin line, right scale; this scale increases downward).

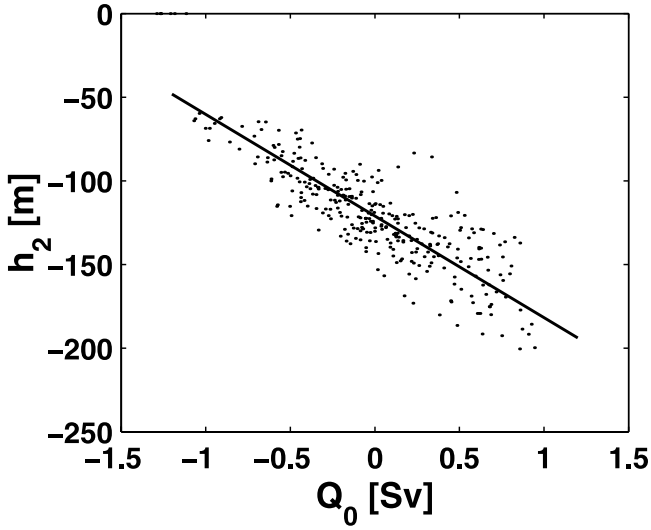

Figure 6. Scatterplot of the interface depth versus the barotropic transport fluctuations. The solid line is the least squares fit.

[34] Differences between $Q_{1U}(t)$ and $Q_{1S}(t)$ (or between $Q_{2U}(t)$ and $Q_{2S}(t)$) can be interpreted in terms of interlayer water exchange or water recirculation, as mentioned in the Introduction. Ideally, time-averaged values of $Q_{1U}(t)$ and $Q_{1S}(t)$ should coincide. In fact, $\overline{Q_{1U}}$ = 0.75 Sv and $\overline{Q_{1S}}$ = 0.73 Sv, in very good agreement (the same applies to $Q_{2U}(t)$ and $Q_{2S}(t)$, obviously). In a hypothetical steady state, water fresher (saltier) than S = 37.77 should be flowing into (out of) the Mediterranean through the eastern section because surfaces of u = 0 and S = 37.77 should coincide. Actually, the mean salinity in u = 0 is S = 37.74, very close to S = 37.77 indeed, but it ranges from 37.05 (8 February 1998) to 38.09 (17 December 1997) following the fluctuations of the net flow (Figure 7). Water whose salinity is within this range may be flowing in either direction, depending on the depth of the surface u = 0 (*zu* hereafter) relative to the depth of S = 37.77 (*zs* hereafter).

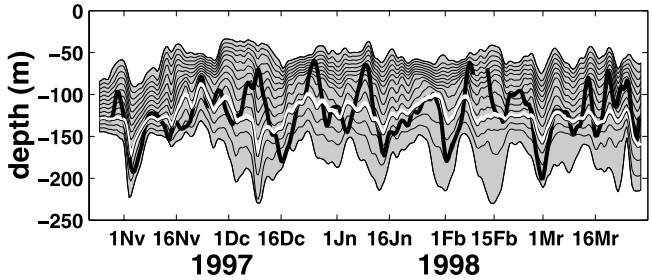

Figure 7. Depth of isohalines from S = 36.8 to S = 38.1 at steps ΔS = 0.1. Thick black line is the depth of u = 0. The thick gray line is the isohaline S = 37.77.

[35] Inflow $Q_{1U}(t)$ and outflow $Q_{2U}(t)$ can be written as

$$Q_{1U} = \int_{zu}^{z=0} (.) = \int_{zu}^{zs} (.) + \int_{zs}^{z=0} (.) = \int_{zu}^{zs} (.) + Q_{1S} \quad (7)$$

$$Q_{2U} = \int_{bottom}^{zu} (.) = \int_{bottom}^{zs} (.) + \int_{zs}^{zu} (.) = \int_{zs}^{zu} (.) + Q_{2S} \quad (8)$$

where (.) stands for $u(z, t)\, dydz$. The difference between inflow and upper layer transport (outflow and lower layer transport) is the term

$$Q_r = \int_{zu}^{zs} u\, dydz \quad \text{if} \quad zs > zu \quad (9)$$

$$Q_r = \int_{zs}^{zu} u\, dydz \quad \text{if} \quad zs < zu \quad (10)$$

that is interpreted as recirculated water. Figure 8 helps clarifying this term. In panel 1, *zu* and *zs* coincide and Q_{1U} and Q_{1S} will also do. In panels 2 and 3, $Q_{1U} > Q_{1S}$ because *zu* and *zs* do not coincide. Case 2 represents an inflow greater than average, whereas case 3 sketches an inflow less than average. In case 2 the layer between *zu* and *zs* (shaded area), which is saltier than 37.77 and therefore belonging to the lower layer, is recirculating toward the Mediterranean. In case 3, the layer between *zs* and *zu* (shaded area) contains water from the upper layer recirculating toward the Atlantic Ocean.

[36] Time series of recirculated water obtained from equations (9) if $zs > zu$ or (10) if $zs < zu$, have been determined and plotted in Figure 9a along with $Q_0(t)$. A correlation coefficient of $r = 0.67$ between Q_r and Q_0 ($r = 0.54$ between Q_r and NPS hindcast net flow) suggests that net flow fluctuations trigger the recirculation of water. Therefore atmospheric forcing would be the ultimate agent driving subinertial recirculation. The obvious physical mechanism will be the enhanced (or diminished) water entrainment produced by the greater (smaller) velocities in the upper layer that would follow a positive (negative) fluctuation of the net flow. Figure 9b shows the good visual

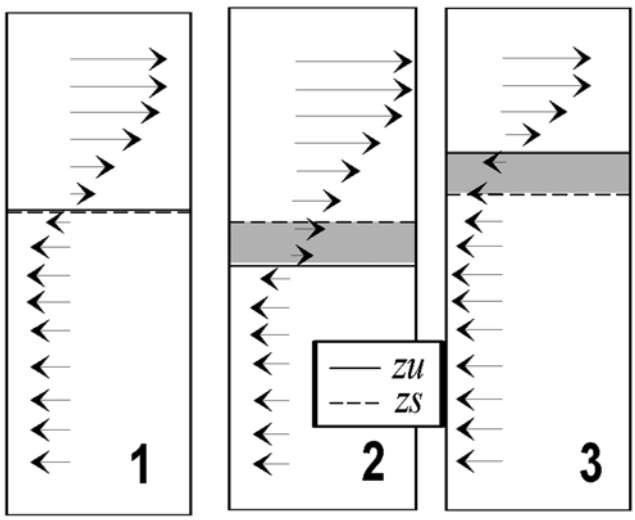

Figure 8. Schematic of recirculation (see text for explanation).

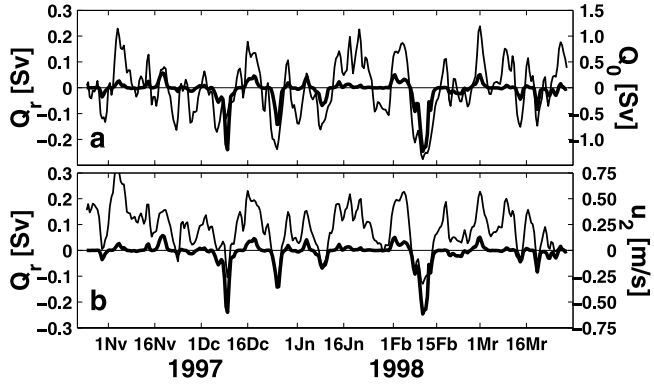

Figure 9. (a) Recirculated water (thick line, left scale) and net flow (thin line, right scale). Note the different scales in the axes. (b) Recirculated water (thick line, left scale) and along strait velocity registered at the nominal depth of −70 m (thin line, right scale).

correlation between Q_r and the along-strait velocity registered at 70 m depth ($r = 0.72$), supporting the very intuitive mechanism commented above.

[37] Vertical excursions of $u = 0$ relative to $S = 37.77$ may surpass 50 m (see Figure 7), implying that water parcels of considerable thickness would be moving back and forth driven by atmospheric fluctuations, thus increasing their residence time within the geographic limits of the strait. In spite of these large vertical excursions Q_r only represents around 5% of Q_0 (Figure 9a) and is small compared to Q_{1S} or Q_{2S}, because water velocity near the surface $u = 0$ is, obviously, very low.

6. Conclusions

[38] Meteorologically induced net flow fluctuations through the Strait of Gibraltar are known to be chiefly driven by atmospheric pressure changes over the Mediterranean Sea. Simple analytical models ignore the effect of wind stress and the variable atmospheric pressure over the Atlantic Ocean on the forced fluctuation. The NPS numerical model applied in this study include both effects. When the model is run forced by the atmospheric pressure uniquely, the results that it provides do not much differ from the results of the simpler analytical model of *Candela et al.* [1989]. The fact that predictions of both models correlate almost equally well with the observed flow indicates that the variable atmospheric pressure over the Atlantic Ocean, which is not included in Candela's model but it is in NPS, is not important to determine the net flow, in agreement with the findings of *Le Traon and Gauzelin* [1997]. It should be mentioned that predictions of both models are less correlated than expected ($r = 0.77$) taking into account that they are forced by (almost) the same external agent.

[39] When wind stress is included in NPS model, the hindcast net flow fluctuations are noticeably improved. Some particular events that are not well hindcast by the model forced by atmospheric pressure alone are much better modelled when including wind stress (see events marked by arrows in Figures 2a and 2b). Figure 2c shows that during these events wind was blowing in the right direction to

achieve this improvement. We speculate that wind-induced setup of sea level at both ends of the strait and/or direct wind stress drag on the sea surface were the likely mechanisms. To this respect it is wind forcing nearby the strait in the open Atlantic Ocean rather than in the semienclosed Mediterranean Sea that influences the net flow fluctuations through the Strait of Gibraltar. Nevertheless, the main subinertial variability is still forced by the atmospheric pressure over the Mediterranean.

[40] The interesting question of how inflow and outflow contribute to the meteorologically driven net fluctuation or, alternately, how they respond to the net barotropic forcing has also been analyzed. Inflow and outflow fluctuates in phase although, on average, $q_1(t)$ contributes by 59% to $Q_0(t)$, that is, around 50% more than $q_2(t)$. Interface (surface of $u = 0$) oscillations at the sampled eastern section correlate quite well with the net barotropic fluctuations with an average gain of −60 m/Sv. These results have been examined within the scope of the two-layer inviscid hydraulic theory to conclude that the exchange is submaximal rather than maximal. However, care is needed to raise definite conclusions because, as pointed out by *Winters and Seim* [2000], mixing and dissipation makes the actual interface of null velocity to be considerable deeper than predicted by the inviscid theory.

[41] To carry out an analysis of some aspects of the exchange directly related to the actual salinity and velocity fields in the eastern section of the strait, we have defined upper and lower layer transports with reference to a material surface. We argued that $S = 37.77$ is the best material surface at the eastern section to separate upper and lower layers. The difference between inflow and upper layer transport (and outflow and lower layer transport) has been explained in terms of water recirculation, Q_r. Fluctuations of the net flow are responsible for the fact that water from the lower layer ($S > 37.77$) that would be flowing toward the Atlantic Ocean flows back toward the Mediterranean from time to time and that water from the upper layer ($S < 37.77$) does similarly toward the Atlantic. The mechanism is the enhanced (or diminished) upper layer velocity associated with positive (or negative) net flow fluctuations (see Figure 9b). While this water recirculation is not important compared with meteorologically induced inflow/outflow fluctuations it may represent an important factor for some biological processes taking place in the strait, like the conveyor-belt-like system discussed by *Echevarria et al.* [2002], and also for the exchanged fluxes of other properties.

[42] **Acknowledgments.** This work was supported by the European Commission through CANIGO project (MAS3-PL95-0443). Partial support by the Spanish National Program of Marine Science and Technology (MAR95-1950-C02-01) is also acknowledged. Thanks are due to the captain and crew of the R/V's *Odón de Buen* from Instituto Español de Oceanografía. We are thankful to Julio Candela for useful discussion on the prediction ability of his model and for providing us with some unpublished results.

References

Álvarez Fanjul, E., B. Pérez Gómez, and I. Rodríguez Sánchez Arévalo, A description of the tides in the eastern North Atlantic, *Prog. Oceanogr.*, *40*, 217–244, 1997.

Álvarez Fanjul, E., B. Pérez Gómez, J. C. Carretero, and I. Rodríguez Sánchez Arévalo, Tide and surge dynamics along the Iberian Atlantic Coast, *Oceanol. Acta*, *21*, 131–143, 1998.

Álvarez Fanjul, E., B. Pérez Gómez, and I. Rodríguez Sánchez Arévalo, NIVMAR: A storm-surge forecasting system for Spanish waters, *Sci. Mar.*, *60*, 145–154, 2001.

Armi, L., and D. M. Farmer, The internal hydraulics of the Strait of Gibraltar and associated sill and narrows, *Oceanol. Acta*, *8*, 37–46, 1985.

Armi, L., and D. M. Farmer, The flow of Mediterranean Water through the Strait of Gibraltar, *Prog. Oceanogr.*, *21*, 1–105, 1988.

Backhaus, J. O., A semi-implicit scheme for the sallow water equations for application to shelf sea modelling, *Cont. Shelf Res.*, *2*, 243–254, 1983.

Backhaus, J. O., and D. Hainbucher, A finite difference general circulation model for shelf sea and its applications to low frequency variability on the North European Shelf, in *Three Dimensional Model of Marine and Estuarine Dynamics*, edited by J. C. Nihoul and B. M. Jamart, Elvesier Oceanogr. Ser., Amsterdam, *45*, 221–244, 1987.

Baringer, M., and J. F. Price, Mixing and spreading of the Mediterranean outflow, *J. Phys. Oceanogr.*, *27*, 1654–1675, 1997.

Bascheck, B., U. Send, J. García Lafuente, and J. Candela, Transport estimates in the Strait of Gibraltar with a tidal inverse model, *J. Geophys. Res.*, *106*, 31,033–31,044, 2001.

Bormans, M., and C. Garrett, The effects of non-rectangular cross-section, friction and barotropic fluctuations on the exchange through the Strait of Gibraltar, *J. Phys. Oceanogr.*, *19*, 1543–1557, 1989.

Bray, N. A., J. Ochoa, and T. H. Kinder, The role of the interface in exchange through the Strait of Gibraltar, *J. Geophys. Res.*, *100*, 10,755–10,776, 1995.

Bryden, H. L., J. Candela, and T. H. Kinder, Exchange through the Strait of Gibraltar, *Prog. Oceanogr.*, *33*, 201–248, 1994.

Candela, J., C. D. Winant, and H. L. Bryden, Meteorologically forced subinertial flows through the Strait of Gibraltar, *J. Geophys. Res.*, *94*, 12,667–12,674, 1989.

Candela, J., C. D. Winant, and A. Ruiz, Tides in the Strait of Gibraltar, *J. Geophys. Res.*, *95*, 7313–7335, 1990.

Charnock, H., Wind stress on a water surface, *Q. J. R. Meteorol. Soc.*, *81*, 639–640, 1955.

Crepon, M., Influence de la pression atmospherique sur le niveau moyen de la Méditerranée Occidentale et sur le flux á travers le Détroit de Gibraltar, *Cah. Oceanogr.*, *1*, 15–32, 1965.

Delgado, J., J. García Lafuente, and J. M. Vargas, A model for submaximal exchange through the Strait of Gibraltar, *Sci. Mar.*, *65*, 313–322, 2001.

Echevarria, F., et al., Physical-biological coupling in the Strait of Gibraltar, *Deep Sea Res., Part II*, *49*, 4115–4130, 2002.

Farmer, D. M., and L. Armi, Maximal two-layer exchange over a sill and through the combination of a sill and contraction with barotropic flow, *J. Fluid Mech.*, *164*, 53–76, 1986.

García Lafuente, J., J. M. Vargas, J. Candela, B. Bascheck, F. Plaza, and T. Sarhan, The tide at the eastern section of the Strait of Gibraltar, *J. Geophys. Res.*, *105*, 14,197–14,213, 2000.

García Lafuente, J., J. Delgado, J. M. Vargas, M. Vargas, F. Plaza, and T. Sarhan, Low frequency variability of the exchanged flows through the Strait of Gibraltar during CANIGO, *Deep Sea Res., Part II*, *49*, 4051–4067, 2002.

Garrett, C., Variable sea level and strait flows in the Mediterranean: A theoretical study of the response to meteorological forcing, *Oceanol. Acta*, *6*, 79–87, 1983.

Garrett, C., The role of the Strait of Gibraltar in the evolution of Mediterranean water, properties and circulation, in *Dynamics of Mediterranean Straits and Channels*, *CIESM Sci. Ser.*, vol. 2, edited by F. Briand, pp. 1–20, Comm. Int. pour l'Explor Sci. de la Mer Mediter., Monaco, 1996.

Garrett, C., and F. Majaess, Nonisostatic response of sea level to atmospheric pressure in the eastern Mediterranean, *J. Phys. Oceanogr.*, *14*, 656–665, 1984.

Le Traon, P. Y., and P. Gauzelin, Response of the Mediterranean mean sea level to atmospheric pressure forcing, *J. Geophys. Res.*, *102*, 973–984, 1997.

Schwiderski, E. W., On charting global ocean tides, *Rev. Geophys.*, *18*, 243–268, 1980.

Send, U., J. Font, G. Krahmann, C. Millot, M. Rhein, and J. Tintoré, Recent advances in observing the physical oceanography of the western Mediterranean Sea, *Prog. Oceanogr.*, *44*, 37–64, 1999.

Tsimplis, M. N., and H. L. Bryden, Estimation of the transports through the Strait of Gibraltar, *Deep Sea Res., Part I*, *47*, 229–2242, 2000.

Winters, K. B., and H. E. Seim, The role of dissipation and mixing in exchange flow through a contracting channel, *J. Fluid Mech.*, *407*, 265–290, 2000.

E. Álvarez Fanjul and A. W. Ratsimandresey, Area del Medio Físico, Puertos del Estado, Avenida del Partenón 10, 28042 Madrid, Spain.

J. García Lafuente and J. M. Vargas, Departamento de Física Aplicada II, E.T.S.I. Telecommunicación, Campus de Teatinos s/n, 29071 Málaga, Spain. (glafuente@ctima.uma.es)